Drivers of forest change in the Greater Yellowstone Ecosystem

Authors: Erika M. Blomdahl[1], James H. Speer[2], Margot Kaye[3], Nicole E. Zampieri[4], Maegen Rochner[5], Bryce Currey[6], Denise Alving[3], Gabriel Cahalan[7], Ben Hagedorn[8], Hang Li[2], Rose Oelkers[9], Lissa Pelletier[10], Ichchha Thapa[2], Kevin Willson[11], Brian D. Woodward[12], R. Justin DeRose[1]

[1] Department of Wildland Resources and Ecology Center, Utah State University, Logan, Utah, USA

[2] Department of Earth and Environmental Systems, Indiana State University, Terre Haute, Indiana, USA

[3] Department of Ecosystem Science and Management, Penn State University, University Park, Pennsylvania, USA

[4] Department of Geography, Florida State University, Tallahassee, Florida, USA

[5] Department of Geographic and Environmental Sciences, University of Louisville, Louisville, Kentucky, USA

[6] Department of Land Resources and Environmental Sciences, Montana State University, Bozeman, Montana, USA

[7] The Nature Conservancy, Arlington, USA

[8] Washington State Department of Natural Resources, Olympia, Washington, USA

[9] Lamont-Doherty Earth Observatory, Columbia University, Palisades, New York, USA

[10] Department of Sustainable Resources Management, SUNY College of Environmental Science and Forestry, Syracuse, New York, USA

[11] Department of Biology, University of New Mexico, Albuquerque, New Mexico, USA

[12] Department of Ecosystem Science and Sustainability, Colorado State University, Fort Collins, Colorado, USA

Correspondence

Erika M. Blomdahl, Department of Wildland Resources and Ecology Center, Utah State University, 5230 Old Main Hill, Logan, Utah 84322-5230, USA

Email: erika.blomdahl@usu.edu

ORCID: Erika M. Blomdahl (https://orcid.org/0000-0002-2614-821X)

Funding

The field week was supported by the National Science Foundation (grant #1759694). This research was supported by the Utah Agricultural Experiment Station, Utah State University, and approved as journal paper number 9453.

Abstract

Context and Questions: Global climate change is predicted to cause widespread shifts in the distribution and composition of forests, particularly in mountain environments where climate exerts strong controls on tree community arrangement. The upslope movement of vegetation has been observed in association with warming temperatures and is especially evident in ecotones—the transition zones between vegetation types. We explored the role of drought and tree mortality on recent changes in high-elevation forests.

Location: Greater Yellowstone Ecosystem, U.S.A.

Methods: We established 19 forest demography plots along an elevational gradient spanning dominant high-elevation vegetation types.

Results: Tree establishment dates indicated the upslope movement of *Pinus albicaulis* (whitebark pine) treeline and ecotone shift from meadow to forest starting in the 1950s. An expansion of the growing season likely contributed to the upward expansion of the treeline. Comparisons between overstory and understory tree composition suggested ongoing succession in the absence of fire at lower elevations, namely the replacement of *Pinus contorta* (lodgepole pine) by *Abies lasiocarpa* (subalpine fir). *P. contorta* seedlings were distributed at higher elevations than overstory trees of the same species, suggesting some potential for upslope movement with warming conditions; *P. albicaulis* seedlings, conversely, were distributed throughout all elevations of the transect. Significant tree mortality occurred in *Pinus* spp. and disproportionately affected *P. albicaulis*, as a result of a regional *Dendroctonus ponderosae* (mountain pine beetle) outbreak (2008-2012). Mortality events were strongly associated with drier than average conditions 2-3 years prior to tree death.

Conclusion: Rising sensitivity to arid conditions in the mid-20th century amid already dense, aging forests appears to have increased susceptibility to beetle-induced mortality during the most recent drought. Tree species in the study area responded individually to global change stressors, which acted on these forests in complex ways and led to both ecotone shifts and stability. This work highlights the interplay between succession, forest disturbances, and climate-related growth responses in driving forest compositional change in subalpine and treeline environments.

Keywords: ecotone shift, mountain pine beetle, climate change, whitebark pine, dendrochronology

Nomenclature: Vegetation: USDA Plants Database (USDA, 2021). Insects: Wood (1982). Birds: Lesica (2002).

1. Introduction

Ongoing climate change has resulted in novel temperature gradients, modified resource availability, and altered disturbance regimes in forested systems across the world (Anderegg et al., 2013; Allen et al., 2015) In high-elevation mixed-conifer forests of North America, mortality events have occurred with increased magnitude and frequency in recent decades (Loehman et al., 2018). While multiple hypotheses exist about the causes of this mortality (Trugman et al., 2021), the specific drivers are likely a complex interaction among temperature stress, moisture stress, and disturbance agents (e.g., insect outbreaks, fire) acting on older and denser forests (Allen et al., 2010; Rocca et al., 2014). Mortality that results from these interactions ranges in intensity from individual trees to entire stands, which can alter forest dynamics depending on stand structure and composition. Increased mortality can also create opportunities for regeneration, migration, and colonization of forest species across spatial scales (Brice et al., 2019).

When new colonization opportunities are presented (e.g., disturbances, tree mortality), a reshuffling of tree species composition could occur (Bell et al., 2014). Models have predicted vegetation shifts poleward and up elevational gradients (e.g., Iverson and McKenzie, 2013), indicating that many vegetation types may experience type conversions as temperatures warm. Examples of poleward and upslope movement of vegetation have already been observed in some forested systems (Johnstone and Chapin, 2003; Beckage et al., 2008; Brashears et al., 2008; Smithers et al., 2018). Given that forests are slowly but continuously changing (Christensen, 2014), identifying climate-driven community shifts of long-lived species is a challenging task.

Shifts in forest composition are thought to be especially evident in ecotones—transition zones between vegetation types (Hufkens et al., 2009)—particularly in mountainous environments where climate can act as a strong control on tree community arrangement (Smith et

al., 2009). In the central Rocky Mountains, the Greater Yellowstone Ecosystem (GYE) includes thousands of hectares of subalpine forest and alpine environments. These systems are characterized by a suite of ecological legacies driven by climate (Krause and Whitlock, 2017), disturbance dynamics (Romme and Despain, 1989; Hatala et al., 2010), and competitive interactions (Tomback et al., 2001a) that act as strong filters for tree species composition. Ecotone shifts have already been observed in some lower-elevation forests of the GYE (Donato et al., 2016), but the role of climate change and disturbance in these shifts remains unresolved.

The principal disturbance agents in the GYE are bark beetle outbreaks, wildfire, and drought. In the early 2000's there was a widespread *Dendroctonus ponderosae* (mountain pine beetle) outbreak in the region, affecting *Pinus albicaulis* (whitebark pine) in particular, with nearly half of the GYE population estimated to have severe tree mortality (Macfarlane et al., 2013). While large *D. ponderosae* outbreaks are a cyclical occurrence in the GYE, the extent and severity of this most recent outbreak was likely amplified by climate change. In high elevation environments, warming temperatures interact with bark beetle dynamics by increasing overwintering survival and larval development rates (Bentz et al., 2010). Water-stressed trees are less able to defend against beetle attack via two main mechanisms: 1) less allocation of secondary metabolites to defense and 2) less hydraulic pressure to pitch out beetles (Franceschi et al., 2005; Anderegg et al., 2015). The period from 2000-2010 has been termed a 'mega-drought' of likely unprecedented severity in the Upper Missouri River Basin, reflecting more arid conditions and reduced snowpack in its headwaters, the Rocky Mountains (Martin et al., 2020). In addition to amplifying bark beetle activity, increased aridity interacts with wildfire frequency and severity. Historical fire regimes in subalpine forests of the interior Rockies are infrequent and mixed- to high-severity, driven by periods of prolonged drought sufficient enough

to dry long-term fuel accumulations (Schoennagel et al., 2004). Fire suppression has altered more historically mixed-severity forest types in the GYE and has likely contributed to the decline of *P. albicaulis* forests (Tomback et al., 2001a).

In this study, we investigated changes in overstory and understory forest composition and structure (i.e., for tree species only) across a 500 m elevational gradient of common forest types in the GYE to determine how and why high-elevation ecotones have changed over the past several decades. Our objective was to characterize the role of drought and recent beetle-caused mortality on possible changes in tree species composition and structure, and determine whether those changes reflect ecotone shifts, successional change, or some combination of both. We analyzed forest and dendrochronological data characterizing species-specific demography to identify species distribution changes and ecotone shifts, expecting upslope movement across all elevations and species, and in particular amongst more drought-sensitive species. We further investigated climate-growth relationships and patterns in tree mortality to help explain observed compositional shifts.

2. Methods

2.1 Study Area

We selected a forested slope on the southwest aspect of South Bird Mountain in the Shoshone National Forest in northwest Wyoming, as our study area (Figure 1). The climate in the region is characterized by a mean annual temperature of 1.2°C, with mean minimum and maximum monthly temperatures of -14.5°C and 22.5°C respectively, and a mean annual precipitation of 775.1 mm (extracted from climateWNA, Wang et al., 2016). The predominant tree species in the study area are *Pinus contorta* (lodgepole pine) and *Pinus albicaulis*, with a lesser component of *Abies lasiocarpa* (subalpine fir), *Picea engelmannii* (Engelmann spruce), and *Pseudotsuga*

menziesii var. *glauca* (Douglas-fir). The transects sampled during the study spanned the following ecotones from lowest (2,558 m) to highest (3,028 m) elevation: sagebrush steppe, *P. contorta*-dominated forest, *P. albicaulis* -dominated forest, and alpine meadow. *P. contorta*-dominated forests initiated in the early-to-mid 19th century, and could be described as late-successional with complex structure and advanced regeneration of shade-tolerant *A. lasiocarpa* in the understory. *P. albicaulis*-dominated forests initiated in the early 19th century and progressively earlier with higher elevations, with early-successional forests above 3000 m. The alpine meadows were sparsely populated with large, dead remnant *P. albicaulis* and *P. engelmannii* stems dating to many centuries ago (Rochner et al., 2021).

[Figure 1 Location]

2.2 Study Design and Data Collection

To assess changes in forest composition, we established two parallel study transects on South Bird Mountain. We used aerial imagery to identify a transect location that appeared representative of the subalpine forests of the GYE and included an elevational gradient of multiple ecotones. We selected a living forested area, thus our scope of inference does not include the post-disturbance dynamics of those 'ghost' forests severely impacted by the bark beetle outbreaks in the early 2000's. The first transect consisted of six plots, ranging in elevation from 2,866 m to 3,006 m, while the second transect consisted of 13 plots, ranging in elevation from 2,561 m to 3,020 m (Figure 1). Plots were spaced 250 m apart across the elevational gradient within each transect. We sampled the first transect in 2017 and the second transect in 2018 and 2019. Of the 19 plots, two were in meadows at the elevational extremes of the transect.

At each forested plot, we measured two forest demographic groups: (1) trees and (2) seedlings and saplings. Trees were defined as stems >5 cm diameter at coring height (DCH) and

158 >1.37 m in height. Seedlings and saplings were defined as stems <5 cm DCH, with saplings
159 >1.37 m in height. We applied *N*-tree distance sampling (Moore, 1954), in which we sampled the
160 10 trees (live or dead) nearest to the plot center. We established each plot radius by measuring
161 from plot center to half the distance between the 10th and 11th trees. Across the dataset, the
162 average forested plot radius was 5.3 m, with radii ranging from 3.8 m to 7.4 m. We identified
163 species and status (e.g., live or dead) for all trees sampled, and recorded observations for canopy
164 position (dominant, codominant, and suppressed) and tree condition (e.g., evidence of bark
165 beetles, fungal fruiting bodies, physical damage). We used increment borers to collect two cores
166 per tree at a coring height of 30 cm. For dead trees that were not sound enough to core, we
167 collected cross-sections. We identified and destructively sampled all seedlings and saplings
168 within the plot radius determined as above.

169 *2.3 Sample Preparation and Tree-Ring Chronologies*

170 We processed increment cores and cross-sections from overstory trees according to
171 standard dendrochronological methods described by Stokes and Smiley (1968) and Speer (2010).
172 Cores were mounted and sanded using progressively finer grit (40, 120, 220, 320, and 400) and
173 finished with 30, 15, and 9 micron sanding film until cell structure was discernible. We
174 developed skeleton plots for a subset of individual series to identify marker years for each
175 species. We then used the memorization method to crossdate the remaining cores (Douglass,
176 1941). Tree-ring widths were measured (resolution: 0.001 mm) using a Velmex TA Measuring
177 Machine with J2X software, and via scanned images (1200 dpi) processed with CooRecorder
178 (Cybis Elektronik, 2010). We statistically validated the visually crossdated cores with
179 COFECHA software (Holmes, 1983). Of the five species present on the study transect, increment
180 core sample depth was large enough to develop final tree-ring chronologies for *P. albicaulis* (142

series from 89 trees) and *P. contorta* (121 series from 66 trees). The expressed population signal for the chronologies used in climatic analyses were 0.92 and 0.89 for the *P. albicaulis* and *P. contorta*, respectively (Table S1). We used an age specific smoothing spline with a fixed stiffness of 30 years to detrend the ontogenetic growth patterns (Klesse, 2021), and autoregressive modeling to remove temporal autocorrelation. All chronology building was done in the R package *dplR* (Bunn, 2008).

To age each of the harvested seedlings and saplings > 30 cm tall, we prepared two cross sections from each sample, one at the base (0 cm height) and another at 30 cm stem height. Seedlings smaller than ~1cm in diameter were cut with a razor blade and the rings were visually counted under a microscope. Cross-sections of seedlings 1-5 cm in diameter were sanded, rings were counted under the microscope, and the memorization method was used to crossdate tree-rings when possible.

2.4 Analytical Approach

2.4.1 Forest Demography

Live and dead trees > 5 cm diameter at coring height (i.e., overstory) were assigned a plot scaling factor based on the radius calculated from the *N*-tree design. Live and dead total basal area, trees per hectare, quadratic mean diameter, and stand density index (Vacchiano et al., 2013) were calculated. Trees per hectare for the understory trees were calculated on a per-species basis using the *N*-tree scaling factor.

Overstory tree cores that intersected the pith were noted, otherwise the number of rings to the pith were estimated using pith locators developed by Applequist (1958). We used the seedling and sapling cross-sections taken at 0 cm and 30 cm to develop an equation for

extrapolating the number of years for a seedling to grow from 0 to 30 cm. We estimated tree establishment year by subtracting the modeled number of years to grow to 30 cm from the pith year measured at 30 cm measurement height. The establishment years of seedlings were the pith year of the cross section at 0 cm.

Dates of tree death were assumed to be the calendar year in which a standing dead tree formed a tree ring. In cases where the latest calendar year did not match across the two core samples for a given tree, the date of death was assigned the most recent year. Additionally, bark beetles (assumed *Dendroctonus ponderosae*) were ascribed as a factor associated with death if blue-stain fungus (assumed one of, *Grosmannia clavigera* Robinson-Jeffrey and Davidson, *Ophiostoma montium* Rumbold, or *Leptographium longiclavatum* S.W. Lee, J.J. Kim & C. Breuil) was present in the sapwood of increment cores of standing dead trees.

2.4.2 Forest Change

We compared patterns of establishment by tree species and status (e.g., live or dead) graphically. To aid graphical interpretation, we binned establishment years into decades, and forested plots into five elevational groups. Elevation bands were assigned by rounding to the nearest 100 m (e.g., "2800 m" includes plots ranging from 2750-2849 m in elevation). To assess possible changes in the distribution and composition of overstory trees relative to understory seedlings and saplings of the same species, we used non-metric multidimensional scaling (NMDS; *vegan* package in *R*; Oksanen et al., 2013) on tree density (stems/ha) by species and form for the 17 forested plots. NMDS results were assessed for the overall reduction of stress. Ordination bi-plots were assessed graphically, and the relationship between NMDS axes (expressed as MDS1 and MDS2) and associated environmental variables were calculated. We then plotted the relative amount of change for each species over the NMDS axes.

2.4.3 Climate Response

To assess relationships between climate variables and the residual chronologies we used response function analyses in the R package *treeclim* (Zang and Biondi, 2015). We explored monthly, seasonal, and water-year responses of tree-ring widths to precipitation, minimum temperature, maximum temperature, and the Palmer Drought Severity Index (PDSI) extracted from the Parameter-elevation Regressions on Independent Slopes Model (PRISM Climate Group, 2020). After preliminary testing, we settled on presenting results for growth responses to monthly minimum and maximum temperature and PDSI using a moving correlation analysis with a 35-year window. We settled on species-specific climate-growth patterns grouped across all elevations because they did not differ substantially when separated into upper and lower elevation groups, perhaps because the majority of stems for each species occurred in a smaller elevational range than the whole transect at large (Figures S1,S2).

To examine possible correspondence of tree mortality with year-to-year drought variability we conducted a superposed epoch analysis (SEA) using tree death dates and historical time series (1895-2019) of summer seasonal drought (June-August) developed from gridded PDSI data (PRISM Climate Group, 2020). We identified 16 unique mortality event years and used the *sea* function in the R package *burnr* (Malevich et al., 2018) to analyze each focal year in relation to the 10 years before and after to test the null hypothesis that drought conditions in the years surrounding a mortality event do not significantly differ from the mean drought conditions over the time period tested (1934-2017).

3. Results

3.1 Forest Demography

We determined establishment dates for 91 *P. albicaulis trees*, 91 *P. contorta trees*, 5 *A. lasiocarpa* trees, 2 *P. engelmannii trees*, and 1 *P. menziesii tree*. Establishment dates of live and dead overstory trees revealed clear successional patterns of species recruitment at lower elevations along our study transect, with stand initiation dominated by *P. contorta* typically followed by establishment of *P. albicaulis* (largely after 1879; Figures 2,S2). Basal area and stem density of *P. contorta* ranged from 2.9 m^2/ha to 51.3 m^2/ha and 163 stems/ha to 720 stems/ha respectively, with the greatest basal area around 2,700 m and the greatest stem density around 2,800 m (Tables 1, 2, S2, S3). Basal area and stem density of *P. albicaulis* ranged from 1.9 m^2/ha to 23.9 m^2/ha and 29 stems/ha to 992 stems/ha respectively, with the greatest basal area around 2,900 m and the greatest stem density around 3,000 m (Tables 1,2, S2, S3). Stocking of *P. albicaulis* and *P. contorta* at all plots was high, with stand density index (SDI) values ranging from 313.7 to 864.5 (Tables 3, S4). *A. lasiocarpa*, *P. engelmannii*, and *P. menziesii* were only minor components of the overstory at all but the highest elevations (Tables 1, 2). Tree establishment year was positively related to elevation, with the oldest trees at the lowest elevations and predominantly younger trees at higher elevations (Figures 2, S3).

[Figure 2 Location]

[Tables 1, 2, and 3 Location]

3.2 Forest Change and Potential Drivers

3.2.1 Ecotone Shift

Age structure and tree species composition of the forest across different elevation bands highlighted areas on the transect where understory communities did not reflect overstory composition. Across the *P. contorta* -dominated stands, 8.5% of total seedling density was *P.*

contorta, while 45.1% was *A. lasiocarpa* and 44.2% was *P. albicaulis*, suggesting the potential for ecotone shift if heterospecific seedlings and saplings accede to the overstory (Figure 2; elevation bands: 2600-2800 m). *P. albicaulis* -dominated stands had similar overstory and understory communities, suggesting relative stability in composition (Figure 2; elevation bands 2900-3000 m)

NMDS ordination comparing densities of overstory trees and understory populations of the same species suggested both stability and the potential for ecotone shift. These populations separated most strongly along the axes of elevation (MDS1, r= -0.85) and total basal area (r= 0.58; Table S5), with a stress of 0.02. Comparisons of MDS1 axis scores between overstory and understory trees of the same species suggested an upslope shift in establishment of *P. contorta* and a downslope shift in *P. albicaulis* (Figure 3). Slight downward shifts were suggested for *A. lasiocarpa*, *P. engelmannii*, and *P. menziesii*; however, these results must be viewed in light of limited tree densities in most plot overstories and some plot understories.

[Figure 3 Location]

We found clear evidence of an ecotone shift in plots greater than 3,000 m in elevation, from meadow to closed-canopy forest. Virtually all of the understory recruitment at the highest elevations occurred in the 20th century, and a substantial majority occurred after 1950 (Figure 4). *P. albicaulis* dominated the understory recruitment signal, in particular at high elevation where it was nearly the only species recruiting.

[Figure 4 Location]

3.2.2 Pine Mortality

Tree mortality across all elevations ranged from 0.4 to 27.2 m^2/ha, was concentrated exclusively in *Pinus* spp. (Tables 1, S2-S4). At higher elevations, 48.0% of the total forest basal

area were *P. albicaulis* standing dead, and at lowest elevations, 37.9% of the total forest basal area was *P. contorta* standing dead (Tables 1, S2). Mortality on the transect disproportionately occurred in *P. albicaulis* (62% of total, compared to 38% of *P. contorta*), where *P. albicaulis* standing dead also tended to be older on average ($p < 0.05$; Figure 5).

[Figure 5 Location]

Drought and *D. ponderosae* were the main drivers of mortality patterns in the study area. Indeed, 42% of mortality events fell within the 2000-2010 time period, characterized as the recent 'mega-drought', and fully 77% died post-2000. Mortality of *Pinus* spp. was largely attributed to the *D. ponderosae* outbreak in 2008-2012. Of the 26 dead trees we were able to assign a year of death, 58% had evidence of blue-stain fungus, 19% did not have blue-stain fungus, and the remainder were undetermined. The average diameter at coring height of beetle-killed *P. contorta* was 29.0 cm, while the average diameter at coring height of beetle-killed *P. albicaulis* was 20.5 cm. Finally, the timing of mortality for the dead trees encountered on the transect was significantly ($p <0.01$) associated with drier than average drought conditions 2-3 years prior to tree death (Figure 6), refuting the null hypothesis that deaths occurred randomly over temporal variability of summer drought.

[Figure 6 Location]

3.2.3 Climate and Tree Growth

Ring-width growth relationships with climate variables suggested both a strengthening of limiting temperature conditions and an emerging and strengthening response to monthly PDSI (Figure 7). Throughout the record, *P. albicaulis* growth had a positive relationship with cool season maximum temperatures. The strength of this relationship was variable but consistent (i.e., positive) over time (Figure 7a). In contrast, *P. contorta* growth had a strong negative response to

316 previous warm season (August and July) monthly maximum temperatures throughout the
317 historical record, indicative of the lagged effect of previous growing season climate conditions
318 on the following growing season, caused by determinate growth (Figure 7b). *P. contorta*
319 exhibited a positive and temporally stable relationship to late-growing season temperature
320 (Figure 7b). Both species exhibited a strengthening positive relationship to previous growing
321 season and fall PDSI in recent decades. The growth response of *P. albicaulis* shifted from a
322 negative to positive relationship with PDSI during the mid-20th century (Figure 7a). *P. contorta*
323 exhibited a negative relationship to current year growing season PDSI in recent decades (Figure
324 7b).
325 [Figure 7 Location]

326 # 4. Discussion

327 Demographic changes and elevational movement in long-lived trees can be challenging
328 to decipher. Pairing forest demographic transects with dendroecological data offers insight into
329 the past and possible future trajectories of the forest when long-term, repeated observations are
330 not available. We measured overstory and understory composition as well as live and dead age
331 structure across a transect spanning 500 m in elevation to assess the potential for ecotone shift in
332 the high elevation forests of the GYE. Trees at the highest elevations (>3000 m) established after
333 1950, indicating ecotone shift from high elevation meadow to *P. albicaulis* -dominated forest.
334 We attribute this shift to an upward advance of *P.albicaulis* rather than regeneration following a
335 mortality event, due to the paucity of dead stems of snags in plots above 3000 m (Tables S2-S4).
336 This shift was synchronous with and positively related to warming winter maximum
337 temperatures, suggesting a relaxing of environmental conditions previously limiting to *P.*

albicaulis establishment. Comparisons between overstory and understory tree composition at different elevational bands suggested compositional stability at higher elevations and ongoing successional patterns in the absence of fire at lower elevations, though our results should be interpreted with the understanding that stochastic effects could influence observed demography at the plot level. Our analysis also revealed that *P. contorta* seedlings were distributed at higher elevations than trees of the same species, which suggested some potential for expected upslope movement with warming conditions. Conversely, *P. albicaulis* seedlings were distributed at lower elevations than *P. albicaulis* overstory trees, possibly a combined result of seed caching and canopy gaps due to extensive tree mortality. At lower elevations dominated by *P. contorta*, about one third of the total basal area were snags that were likely created via drought- and beetle-caused mortality exacerbated by warming temperatures and higher stand densities. At higher elevations mortality on the transect was greatest in *P. albicaulis* -dominated stands, despite lower stand densities. This combined with snag age structure reflects a disproportionate level of mortality amongst old *P. albicaulis* trees.

4.1 Vegetation Change and Potential Drivers

4.1.1 Ecotone Shift

Differences between overstory and advanced regeneration composition may approximate ecotone shifts in GYE subalpine forests. If current disturbance and climate trends continue, we expect understory seedling composition to estimate future overstory composition as fire exclusion, warmer temperatures, greater aridity, and bark beetle attacks shape recruitment into the canopy. Aging *P. contorta* stands, which typically establish after stand-replacing disturbances such as wildfire, are being predictably replaced by *A. lasiocarpa* and *P. albicaulis*,

and to a lesser extent, *P. engelmannii* and *P. menziesii* (Figure 2). We speculate that high stand densities created conditions less favorable for shade-intolerant *P. contorta* seedlings and more favorable for shade-tolerant *A. lasiocarpa* seedlings as predicted by successional theory (Clements, 1910). This is consistent with the findings of Chai et al. (2019) and Brice et al. (2019), who demonstrated the replacement of shade-intolerant pioneer species by shade-tolerant species in the absence of disturbance via a different study design involving permanent plots with multiple censuses. The distribution of *P. contorta* also appears to be moving upslope (Figure 3), coincident with elevated levels of *P. albicaulis* mortality that created light gaps in the canopy at higher elevations (Table 1).

In contrast, *P. albicaulis* may establish in denser forests at lower elevations, in large part due to dissemination from Clark's nutcracker. Goeking and Izlar (2018) found that the majority of *P. albicaulis* stems in the western U.S. occur in forest types dominated by other species, including the forest types: *P. contorta*; spruce-fir; *A. lasiocarpa*; *P. menziesii*; nonstocked (< 10% of full stocking of live trees), and *P. engelmannii*. However, *P. albicaulis* seedlings are less shade tolerant than *A. lasiocarpa* (Minore, 1979), so long-term survivorship may be expected to be lower in most areas on our study transect except for the young, sparse, leading edge of *P. albicaulis* stands. These successional processes, as well as climate trends and disturbances like bark beetle outbreaks and fire will likely dictate which understory trees accede to the canopy in future forests.

The upward expansion of *P. albicaulis* forest into high elevation meadows is likely a consequence of changing climate and fire suppression. We posit that a general warming trend that started around the mid-twentieth century has allowed for *P. albicaulis* establishment. Increasing winter temperatures were also positively correlated with *P. albicaulis* growth,

possibly due to accelerated snowmelt and expansion in the length of the growing season. This is consistent with other studies that have related the expansion of forest treeline to warming climate (e.g., Klasner and Fagre, 2002; Millar et al., 2008; Kullman, 2016). However, Schrag et al. (2008) modeled a decrease in treeline *P. albicaulis* under climate change scenarios of a 4.5°C increase in temperature and a 35% increase in precipitation, suggesting a climate envelope that would eventually inhibit expansion at treeline. We also suspect that 20th century fire suppression played a role in limiting fire in the region that encouraged greater seedling establishment rates in our transects during this period (Brown et al., 2020). The lack of fire may have also played a role in the ecotone shift we observed, as young trees are unlikely to survive fire of any severity.

4.1.2 Pine Mortality

Patterns in stand density generally coincided with areas of high mortality across the two transects. Observed densities suggested imminent density-dependent mortality at all but the highest elevations (i.e., stand density of *P. contorta* stands >420; McCarter and Long, 1986; stand density of *P. albicaulis* stands >370; Shaw, 2017). High densities create stressful competitive environments that increase the risk of spread of biotic disturbance agents such as bark beetles (Perkins and Roberts, 2003; Das et al., 2011). Mortality, largely due to *D. ponderosae*, was high at the lowest elevations characterized by a *P. contorta* overstory and high stand density index (Table 3). In lower-density, higher elevation *P. albicaulis* stands, mortality was better explained by drought stress in conjunction with *D. ponderosae* activity. Despite seemingly better growing conditions, areas converted from alpine meadow to *P. albicaulis* forest experienced mortality in nearly half the total stand basal area (Table 1).

The results of the SEA suggest a drought-driven mortality spiral for the *Pinus* spp. in this study (Figure 6). Though the 'fading record' of long dead trees that decomposed prior to this

study limits our inference to more recent decades, it is notable that nearly half of the mortality events we observed fell within the 2000-2010 time period, characterized as the recent 'mega-drought' (Martin et al., 2020). Given that *D. ponderosae* has a one-year life cycle and takes several years to build to epidemic levels, (Bentz and Powell, 2014) the 2-3-year lag between extremely dry conditions and mortality suggests that these trees died from the combined pressure of drought and *D. ponderosae* attack. Drought can act in dual capacity to enable tree death: 1) reducing host vigor due to increased vapor pressure deficit, and lower soil moisture available to trees, and 2) by increasing the population of the ultimately poikilothermic bark beetles. This lag in timing between tree death and environmental variability has been found for other *D. ponderosae* hosts (e.g., Boutte et al., 2016), and also for other *Dendroctonus* spp. host species like *P. engelmannii* (Mast and Veblen, 1994; DeRose and Long, 2012; DeRose et al., 2017).

4.1.3 Climate and Tree Growth

Warming temperatures and drought both played a role in forest change in the GYE. Correlations between radial growth and climate suggested an increasingly positive relationship to monthly maximum temperature in *P. albicaulis*, coincident with an expansion of the *P. albicaulis* treeline since 1950. This observation follows expectations, as tree growth in subalpine elevations was historically constrained by the length of the growing season and snow cover (Peterson, 1998). Mid-twentieth century, *P. albicaulis* growth switched from a negative to a positive relationship with PDSI (negative values correspond to drier conditions), suggesting a switch to a more limiting, arid environment following an especially long, cool period (Rochner et al., 2021). For both *P. albicaulis* and *P. contorta* the positive relationship to previous growing season PDSI strengthened in recent decades, likely exacerbating the *Pinus* spp. mortality during the 2008-2012 *D. ponderosae* outbreak. *P. contorta* growth also had a negative relationship to

current growing season PDSI in recent decades, a counterintuitive finding that merits further inquiry. Interestingly, the high elevation changes in *P. albicaulis* that we have observed on our transect may be a relatively short-term snippet of a multi-centennial shift in ecotones that often occurs in harsh environments. Upslope of our transects, extensive *P. albicaulis* and *P. engelmannii* forest existed until the middle-to-late part of the Little Ice Age (Rochner et al., 2021). Recruitment of these forests occurred nearly 1,000 years ago, but experienced widespread die-off in the mid-1800s during the coolest conditions of the last millennium, putatively due to climatic causes (Rochner et al., 2021).

4.2 Implications for P. albicaulis Decline

The decline of *P. albicaulis* in the GYE has been the cause of much concern in recent decades (Tomback et al., 2001b; Keane et al., 2017; Goeking and Izlar, 2018), leading the US Fish and Wildlife Service to propose it be listed as threatened under the Endangered Species Act in December 2020. *P. albicaulis* is considered a keystone species because it promotes biodiversity by providing habitat to many species and a central food source via its large, nutritious seeds (Tomback and Kendall, 2001). Given recent declines and ongoing climate change, studies that assess *P. albicaulis* stability and upslope movement are important to help managers target restoration efforts. We found a disproportionate level of mortality in *P. albicaulis* in our study area, with virtually all mortality events attributable to *D. ponderosae*. While we did not make explicit comparisons (e.g., genetics) between living and dead *P. albicaulis*, death dates suggested that climate change-driven drought played a role in creating conditions that resulted in elevated beetle-related mortality (Six et al., 2018). Despite the elevated levels of mortality in mature trees, there was substantial *P. albicaulis* in the understory, some of which was making its way into the

high elevation meadows. The slow march toward higher elevations could portend the return of *P. albicaulis* to a niche it realized prior to the Little Ice Age cooling (Rochner et al., 2021).

5. Conclusions

We observed a forest undergoing compositional change across different elevations, mediated by an interplay of climate-related stressors, bark beetle outbreak, and successional processes. Non-stable temperatures and increased sensitivity to aridity during the mid-20th century, in combination with increasing stand density associated with aging forests, likely created conditions of increased susceptibility to beetle-induced mortality during the most recent two decades. In the context of these compound stressors, forest age, structure, and composition sampled across an elevational gradient suggested evidence for both ecotone shifts for some species and stability for others. Our assessment of tree species movement in the context of climate change and disturbance history advances understanding of the drivers of tree community change in the subalpine forests of the GYE.

Acknowledgements

This paper was prepared, in part, as participants in the North American Dendro-Ecological Fieldweek (2017, 2018, and 2019) and we would like to thank the additional students who contributed to field data collection.

Author contributions

EMB, JHS, MK, and MR conceived of the research idea and methodology; all authors collected the data; EMB, JHS, NEZ, BC, GC, BH, HL, RO, LP, IT, KW, and RJD performed statistical

analyses; EMB, RJD, and BDW wrote the paper with contributions from all KW and DA; all authors discussed the results and commented on the manuscript.

Data availability statement

All data and script used to produce this manuscript are available upon request from the corresponding author.

References

Allen, C.D., Breshears, D.D. and McDowell, N.G. (2015) On underestimation of global vulnerability to tree mortality and forest die-off from hotter drought in the Anthropocene. *Ecosphere*, 6(8), 1–55. https://doi.org/10.1890/ES15-00203.1.

Allen, C.D., Macalady, A.K., Chenchouni, H., Bachelet, D., McDowell, N., Vennetier, M., et al. (2010) A global overview of drought and heat-induced tree mortality reveals emerging climate change risks for forests. *Forest Ecology and Management*, 259(4), 660–684. https://doi.org/10.1016/j.foreco.2009.09.001.

Anderegg, W.R.L., Hicke, J.A., Fisher, R.A., Allen, C.D., Aukema, J., Bentz, B., et al. (2015) Tree mortality from drought, insects, and their interactions in a changing climate. *New Phytologist*, 208(3), 674–683. https://doi.org/10.1111/nph.13477.

Anderegg, W.R.L., Kane, J.M. and Anderegg, L.D. (2013) Consequences of widespread tree mortality triggered by drought and temperature stress. *Nature Climate Change*, 3(1), 30–36. https://doi.org/10.1038/nclimate1635.

490 Applequist, M. (1958) A simple pith locator for use with off-center increment cores. *Journal of*
491 *Forestry*, 56(1), 141.

492 Beckage, B., Osborne, B., Gavin, D.G., Pucko, C., Siccama, T. and Perkins, T. (2008) A rapid
493 upward shift of a forest ecotone during 40 years of warming in the Green Mountains of Vermont.
494 *Proceedings of the National Academy of Sciences*, 105(11), 4197–4202.
495 https://doi.org/10.1073/pnas.0708921105.

496 Bell, D.M., Bradford, J.B. and Lauenroth, W. (2014) Early indicators of change: divergent
497 climate envelopes between tree life stages imply range shifts in the western United States.
498 *Global Ecology and Biogeography*, 23(2), 168–180. https://doi.org/10.1111/geb.12109.

499 Bentz, B.J. and Powell, J.A. (2014) Mountain pine beetle seasonal timing and constraints to
500 bivoltinism (A comment on Mitton and Ferrenberg, 'Mountain pine beetle develops an
501 unprecedented summer generation in response to climate warming'). *The American Naturalist*,
502 184(6), 787–796. https://doi.org/10.1086/678405.

503 Bentz, B.J., Regniere, J., Fettig, C.J., Hansen, M., Hayes, J.L., Hicke, J.A., et al. (2010) Climate
504 change and bark beetles of the western United States and Canada: direct and indirect effects.
505 *BioScience*, 60(8), 602–613. https://doi.org/10.1525/bio.2010.60.8.6.

506 Boutte, P.C., Hicke, J.A., Preisler, H.K., Abatzoglou, J.T., Raffa, K.F. and Logan, J.A. (2016)
507 Climate influences on whitebark pine mortality from mountain pine beetle in the Greater
508 Yellowstone Ecosystem. *Ecological Applications*, 26(8), 2507–2524.
509 https://doi.org/10.1002/eap.1396.

Breshears, D.D., Huxman, T.E., Adams, H.D., Zou, C.B., and Davison, J.E.. (2008) Vegetation synchronously leans upslope as climate warms. *Proceedings of the National Academy of Sciences,* 105(33): 11591-11592. 10.1073/pnas.0806579105.

Brice, M.H., Cazelles, K., Legendre, P. and Fortin, M.J. (2019) Disturbances amplify tree community responses to climate change in the temperate-boreal ecotone. *Global Ecology and Biogeography*, 28(11), 1668–1681. https://doi.org/10.1111/geb.12971.

Brown, S.R., Baysinger, A., Brown, P.M., Cheek, J.L., Diez, J.M., Gentry, C.M., et al. (2020) Fire history across forest types in the southern Beartooth Mountains, Wyoming. *Tree-Ring Research*, 76(1), 27–39. https://doi.org/10.3959/TRR2018-11.

Bunn, A.G. (2008) A dendrochronology program library in R (dplR). *Dendrochronologia*, 26(2), 115–124. https://doi.org/10.1016/j.dendro.2008.01.002.

Chai, R.K., Andrus, R.A., Rodman, K., Harvey, B.J., and Veblen, T.T. (2017) Stand dynamics and topographic setting influence changes in live tree biomass over a 34-year permanent plot record in a subalpine forest in the Colorado Front Range. *Canadian Journal of Forest Research*, 49: 1256-1264. https://doi.org/10.1139/cjfr-2019-0023

Christensen, N.L. (2014) An historical perspective on forest succession and its relevance to ecosystem restoration and conservation practice in North America. *Forest Ecology and Management*, 330, 312–322. https://doi.org/10.1016/j.foreco.2014.07.026.

Clements, F.E. (1910). The life history of lodgepole burn forests. *USDA For. Serv. Bull.* 79: 7–56.

Cybis Elektronik (2010) *CDendro and CooRecorder*. Available at: http://www.cybis.se/forfun/dendro/index.htm.

Das, A., Battles, J., Stephenson, N.L. and van Mantgem, P.J. (2011) The contribution of competition to tree mortality in old-growth coniferous forests. *Forest Ecology and Management*, 261(7), 1203–1213. https://doi.org/10.1016/j.foreco.2010.12.035.

DeRose, R.J., Bekker, M.F. and Long, J.N. (2017) Traumatic resin ducts as indicators of bark beetle outbreaks. *Canadian Journal of Forest Resources*, 47, 1168–1174. http://dx.doi.org/10.1139/cjfr-2017-0097.

DeRose, R.J. and Long, J.L. (2012) Drought-driven disturbance history characterizes a southern Rocky Mountain subalpine forest. *Canadian Journal of Forest Resources*, 42, 1649–1660. doi:10.1139/X2012-102.

Donato, D.C., Harvey, B.J., and Turner, M.G.. (2016) Regeneration of montane forests 24 years after the 1988 Yellowstone fires: A fire-catalyzed shift in lower treelines? *Ecosphere*, 7(8), e01410. https://doi.org/10.1002/ecs2.1410.

Douglass, A.E. (1941) Crossdating in dendrochrology. *Journal of Forestry*, 39(10), 825–831. https://doi.org/10.1093/jof/39.10.825.

Franceschi, V.R., Krokene, P., Christiansen, E. and Krekling, T. (2005) Anatomical and chemical defenses of conifer bark against bark beetles and other pests. *New Phytologist*, 167(2), 353–376. https://doi.org/10.1111/j.1469-8137.2005.01436.x.

549 Goeking, S.A. and Izlar, D.K. (2018) Pinus albicaulis Engelm. (whitebark pine) in mixed-species
550 stands throughout its US range: broad-scale indicators of extent and recent decline. *Forests*, 9(3),
551 131. https://doi.org/10.3390/f9030131.

552 Hatala, J.A., Crabtree, R.L., Halligan, K.Q. and Moorcroft, P.R. (2010) Landscape-scale patterns
553 of forest pest and pathogen damage in the Greater Yellowstone Ecosystem. *Remote Sensing of*
554 *Environment*, 114(2), 375–384. https://doi.org/10.1016/j.rse.2009.09.008.

555 Holmes, R.L. (1983) Computer-assisted quality control in tree-ring dating and measurement.
556 *Tree-Ring Bulletin*, 43, 69–78.

557 Hufkens, K., Scheunders, P., and Ceulemans, R. (2009) Ecotones in vegetation ecology:
558 methodologies and definitions revisited. *Ecological Research*, 24, 977-986.
559 https://doi.org/10.1007/s11284-009-0584-7

560 Iverson, L.R. and McKenzie, D. (2013) Tree-species range shifts in a changing climate:
561 detecting, modeling, assisting. *Landscape Ecology*, 28(5), 879–889.
562 https://doi.org/10.1007/s10980-013-9885-x.

563 Johnstone, J.F. and Chapin, F.S. (2003) Non-equilibrium succession dynamics indicate continued
564 northern migration of lodgepole pine. *Global Change Biology*, 9(10), 1401–1409.
565 https://doi.org/10.1046/j.1365-2486.2003.00661.x.

566 Keane, R., Holsinger, L., Mahalovich, M. and Tomback, D. (2017) *Restoring whitebark pine*
567 *ecosystems in the face of climate change.* General Technical Report RMRS-GTR-361. Fort
568 Collins, CO: US Department of Agriculture, Forest Service, Rocky Mountain Research Station.,
569 123.

570 Klasner, F.L., and Fagre, D.B. (2018) A Half Century of Change in Alpine Treeline Patterns at
571 Glacier National Park, Montana, U.S.A. *Arctic, Antarctic, and Alpine Research* 34(1), 49-56.
572 https://doi.org/10.1080/15230430.2002.12003468

573 Klesse, S. 2021. Critical note on the application of the "two-third" spline. Dendrochronologia 65,
574 125786. https://doi.org/10.1016/j.dendro.2020.125786

575 Krause, T.R. and Whitlock, C. (2017) Climatic and non-climatic controls shaping early
576 postglacial conifer history in the northern Greater Yellowstone Ecosystem, USA. *Journal of*
577 *Quaternary Science*, 32(7), 1022–1036. https://doi.org/10.1002/jqs.2973.

578 Kullman, L. (2016) Climate Change and Primary Birch Forest (Betula pubescensssp.
579 czerepanovii) Succession in the Treeline Ecotone of the Swedish Scandes. *International Journal*
580 *of Research in Geography* 2(2), 36-47. http://dx.doi.org/10.20431/2454-8685.0202004

581 Loehman, R.A., Bentz, B.J., DeNitto, G.A., Keane, R.E., Manning, M.E., Duncan, J.P., et al.
582 (2018) Effects of climate change on ecological disturbance in the Northern Rockies. In: *Climate*
583 *change and Rocky Mountain ecosystems.* Springer, Cham, pp. 115–141.

584 Macfarlane, W.W., Logan, J.A. and Kern, W.R. (2013) An innovative aerial assessment of
585 Greater Yellowstone Ecosystem mountain pine beetle-caused whitebark pine mortality.
586 *Ecological Applications*, 23(2), 421–437. https://doi.org/10.1890/11-1982.1.

587 Malevich, S.B., Guiterman, C.H. and Margolis, E.Q. (2018) burnr: Fire history analysis and
588 graphics in R. *Dendrochronologia*, 49, 9–15. https://doi.org/10.1016/j.dendro.2018.02.005.

589 Martin, J.T., Pederson, G.T., Woodhouse, C.A., Cook, E.R., McCabe, G.J., Anchukaitis, K.J., et
590 al. (2020) Increased drought severity tracks warming in the United States' largest river basin.
591 *Proceedings of the National Academy of Sciences*, 117(21), 11328–11336.
592 https://doi.org/10.1073/pnas.1916208117.

593 Mast, J.N. and Veblen, T.T. (1994) A dendrochronological method of studying tree mortality
594 pattern. *Physical Geography*, 15(6), 529–542. https://doi.org/10.1080/02723646.1994.10642533.

595 McCarter, J.B. and Long, J.N. (1986) A lodgepole pine density management diagram. *Western*
596 *Journal of Applied Forestry*, 1(1), 6–11. https://doi.org/10.1093/wjaf/1.1.6.

597 Millar, C.I, Westfall, R.D., Delaney, D.L., King, J.C., and Graumlich, L.J. (2001) Response of
598 Subalpine Conifers in the Sierra Nevada, California, U.S.A., to 20th-Century Warming and
599 Decadal Climate Variability. *Arctic, Antarctic, and Alpine Research* 36(2), 181-200.
600 DOI:10.1657/1523-0430(2004)036[0181:ROSCIT]2.0.CO;2

601 Minore, D. (1979) *Comparative autecological characteristics of northwestern tree species: a*
602 *literature review*. General Technical Report PNW-87. Portland, Oregon: US Department of
603 Agriculture, US Forest Service, Pacific Northwest Forest and Range Experiment Station.

604 Moore, P. (1954) Spacing in Plant Populations. *Ecology*, 35(2), 222–227.
605 https://doi.org/10.2307/1931120.

606 Oksanen, J., Blanchet, F.G., Friendly, M., Kindt, R., Legendre, P., McGlinn, D., et al. (2013)
607 *Vegan: community ecology package. Version 2.4-5*. Available at: http://cran.r-
608 project.org/package=vegan [Accessed: 5 December 2021].

609 Perkins, D. and Roberts, D. (2003) Predictive models of whitebark pine mortality from mountain
610 pine beetle. *Forest Ecology and Management*, 174(1–3), 495–510.
611 https://doi.org/10.1016/S0378-1127(02)00066-X.

612 Peterson, D.L. (1998) Climate, limiting factors and environmental change in high-altitude forests
613 of Western North America. In: *The impacts of climate variability on forests.* Springer, Berlin,
614 Heidelberg (Lecture Notes in Earth Sciences), pp. 191–208.

615 PRISM Climate Group (2020) *Climatological normals, 1981-2010*.

616 Rocca, M.E., Brown, P.M., MacDonald, L.H. and Carrico, C.M. (2014) Climate change impacts
617 on fire regimes and key ecosystem services in Rocky Mountain forests. *Forest Ecology and*
618 *Management*, 327, 290–305. https://doi.org/10.1016/j.foreco.2014.04.005.

619 Rochner, M.L., Heeter, K.J., Harley, G.L., Bekker, M.F. and Horn, S.P. (2021) Climate-induced
620 treeline mortality during the termination of the Little Ice Age in the Greater Yellowstone
621 Ecoregion, USA. *The Holocene*, 31(8), 1288–1303.
622 https://doi.org/10.1177/09596836211011656.

623 Romme, W.H. and Despain, D.G. (1989) Historical perspective on the Yellowstone fires of
624 1988. *Oxford Journals*, 39(10), 695–699. https://doi.org/10.2307/1311000.

625 Schoennagel, T., Veblen, T.T. and Romme, W.H. (2004) The interaction of fire, fuels, and
626 climate across Rocky Mountain forests. *BioScience*, 54(7), 661–676.
627 https://doi.org/10.1641/0006-3568(2004)054[0661:TIOFFA]2.0.CO;2.

628 Schrag, A.M., Bunn, A.G., and Graumlich, L.J.(2007) Influence of bioclimatic variables on tree-
629 line conifer distribution in the Greater Yellowstone Ecosystem: implications for species of
630 conservation concern. *Journal of Biogeography* 35, 698–710. https://doi.org/10.1111/j.1365-
631 2699.2007.01815.x

632 Shaw, J.D. (2017) *National determination of maximum stand density index from Forest*
633 *Inventory and Analysis plots*. Ogden, UT: Unpublished report on file at: U.S. Department of
634 Agriculture, Forest Service, Rocky Mountain Research Station.

635 Six, D.L., Vergobbi, C. and Cutter, M. (2018) Are survivors different? Genetic-based selection
636 of trees by mountain pine beetle during a climate change-driven outbreak in a high-elevation
637 pine forest. *Frontiers in Plant Science*, 9, 993. https://doi.org/10.3389/fpls.2018.00993.

638 Smith, W.K., Germino, M.J., Johnson, D.M. and Reinhardt, K. (2009) The altitude of alpine
639 treeline: a bellwether of climate change effects. *The Botanical Review*, 75, 163–190.
640 https://doi.org/10.1007/s12229-009-9030-3.

641 Smithers, B.V., North, M.P., Millar, C.I. and Latimer, A.M. (2018) Leap frog in slow motion:
642 Divergent responses of tree species and life stages to climatic warming in Great Basin subalpine
643 forests. *Global Change Biology*, 24(2), e442–e457. https://doi.org/10.1111/gcb.13881.

644 Speer, J.H. (2010) *Fundamentals of tree-ring research*. University of Arizona Press.

645 Stokes, M.A. and Smiley, T.L. (1968) *An introduction to tree-ring dating*. Chicago, Illinois:
646 University of Chicago Press.

Tomback, D.F., Anderies, A.J., Carsey, K.S., Powell, M.L. and Mellmann-Brown, S. (2001) Delayed seed germination in whitebark pine and regeneration patterns following the Yellowstone fires. *Ecology*, 82(9), 2587–2600. https://doi.org/10.1890/0012-9658(2001)082[2587:DSGIWP]2.0.CO;2.

Tomback, D.F., Arno, S.F. and Keane, R.E. (eds) (2001) *Whitebark pine communities: ecology and restoration*. Island Press.

Tomback, D.F. and Kendall, K.C. (2001) Biodiversity losses: the downward spiral. In: Tomback, D.F., Arno, S.F., and Keane, R.E. (Eds), *Whitebark pine communities: ecology and restoration*. Washington DC: Island Press, pp. 243–262.

Trugman, A.T., Anderegg, L.D., Anderegg, W.R., Das, A.J. and Stephenson, N.L. (2021) Why is tree drought mortality so hard to predict? *Trends in Ecology and Evolution*, 36(6), 520–532. https://doi.org/10.1016/j.tree.2021.02.001.

Vacchiano, G., Derose, R.J., Shaw, J.D., Svoboda, M. and Motta, R. (2013) A density management diagram for Norway spruce in the temperate European montane region. *European Journal of Forest Research*, 132(3), 535–549. https://doi.org/10.1007/s10342-013-0694-1.

Wang, T., Hamann, A., Spittlehouse, D. and Carroll, C. (2016) Locally downscaled and spatially customizable climate data for historical and future periods for North America. *Plos One*, 11(6), e0156720. https://doi.org/10.1371/journal.pone.0156720.

Zang, C. and Biondi, F. (2015) treeclim: an R package for the numerical calibration of proxy-climate relationships. *Ecography*, 38(4), 431–436. https://doi.org/10.1111/ecog.01335.

Tables and Figures

TABLE 1. Average live and dead basal area (m^2/hectare) for all trees in the study transect > 5 cm diameter at coring height, grouped by elevation band. Species codes: ABLA: *Abies lasiocarpa*; PIAL: *Pinus albicaulis*; PICO: *Pinus contorta*; PIEN: *Picea engelmannii*; PSME: *Pseudotsuga menziesii*.

Elev. Band	**Live basal area** (m^2/ha) (percent of total live)						**Dead basal area** (m^2/ha) (percent of total live + dead)	
	ABLA	PIAL	PICO	PIEN	PSME	Total	PIAL	PICO
3000	0 (0)	9 (77.6)	2.6 (22.4)	0 (0)	0 (0)	11.6	10.9 (48)	0.2 (0.9)
2900	0 (0)	23.9 (80.2)	4.7 (15.8)	1.2 (4)	0 (0)	29.8	13.5 (31.2)	0 (0)
2800	0 (0)	4.1 (9.6)	36.6 (86.1)	1.2 (2.8)	0.6 (1.4)	42.5	0 (0)	9.8 (18.7)
2700	0 (0)	2.8 (5.2)	51.3 (94.8)	0 (0)	0 (0)	54.1	0 (0)	0.4 (0.7)
2600	5.7 (12.8)	1.9 (4.3)	36.9 (82.9)	0 (0)	0 (0)	44.5	0 (0)	27.2 (37.9)
Avg:	1.1	8.3	26.4	0.5	0.1	36.5	4.9	7.5

673 **TABLE 2** Average live and dead stem densities (trees/hectare) for all trees in the study transect
674 > 5 cm diameter at coring height, grouped by elevation band. Species codes: ABLA: *Abies*
675 *lasiocarpa*; PIAL: *Pinus albicaulis*; PICO: *Pinus contorta*; PIEN: *Picea engelmannii*; PSME:
676 *Pseudotsuga menziesii*.

	Live stem density (trees/ha)						**Dead stem density (trees/ha)**		
Elev. Band	ABLA	PIAL	PICO	PIEN	PSME	Total	PIAL	PICO	Total
3000	0	992	169	0	0	1160	271	23	294
2900	0	775	163	38	0	1002	343	0	343
2800	0	337	720	32	36	1124	0	85	85
2700	0	346	626	0	0	972	0	48	48
2600	388	29	586	0	0	1004	0	388	388
Avg:	78	496	453	14	7	1052	123	109	232

677

678 **TABLE 3** Average stand density index (SDI), quadratic mean diameter (QMD), live and dead
679 basal area (BA; m^2/hectare), and live and dead stem density (trees/hectare) for all trees in the
680 study transect > 5 cm diameter at coring height, grouped by elevation band.

Elev. Band	SDI	QMD	Live BA	Dead BA	Live Density	Dead Density
3000	313.7	12	11.6	11.2	1160	294
2900	614.1	19.7	29.9	13.5	1002	343
2800	828.9	21.8	42.4	9.8	1124	85
2700	961	24.4	54.2	0.4	972	48
2600	864.5	25.5	44.4	27.2	1004	388
Avg:	664.2	19.6	33.1	12.1	1065	241

681

682

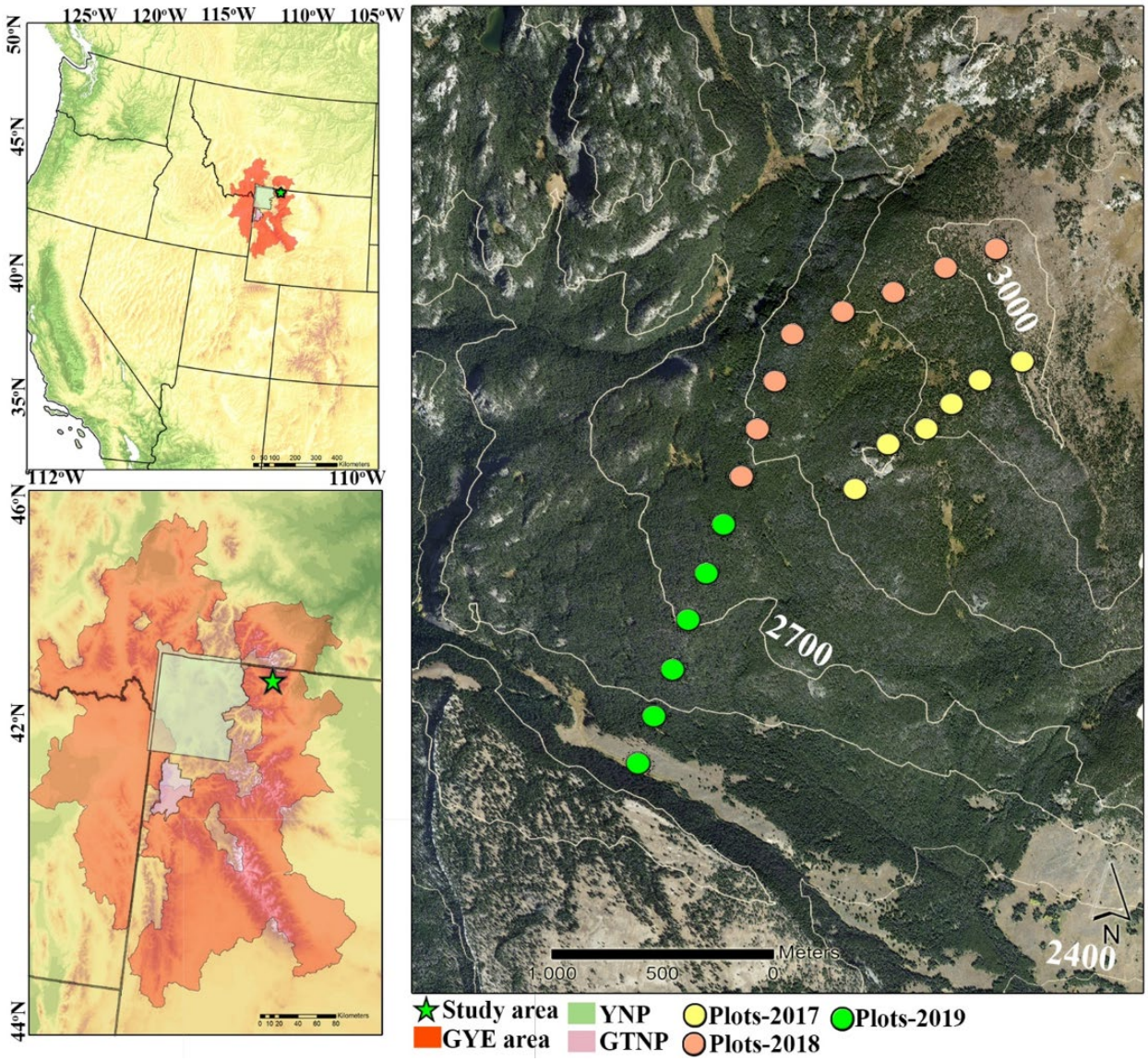

683 **FIGURE 1** The location of the study transect in relation to Grand Teton National Park (GTNP),
684 Yellowstone National Park (YNP), and the Greater Yellowstone Ecosystem (GYE). The transect
685 spans a 500 m elevational gradient and was sampled over a 3-year period, from 2017 to 2019.
686

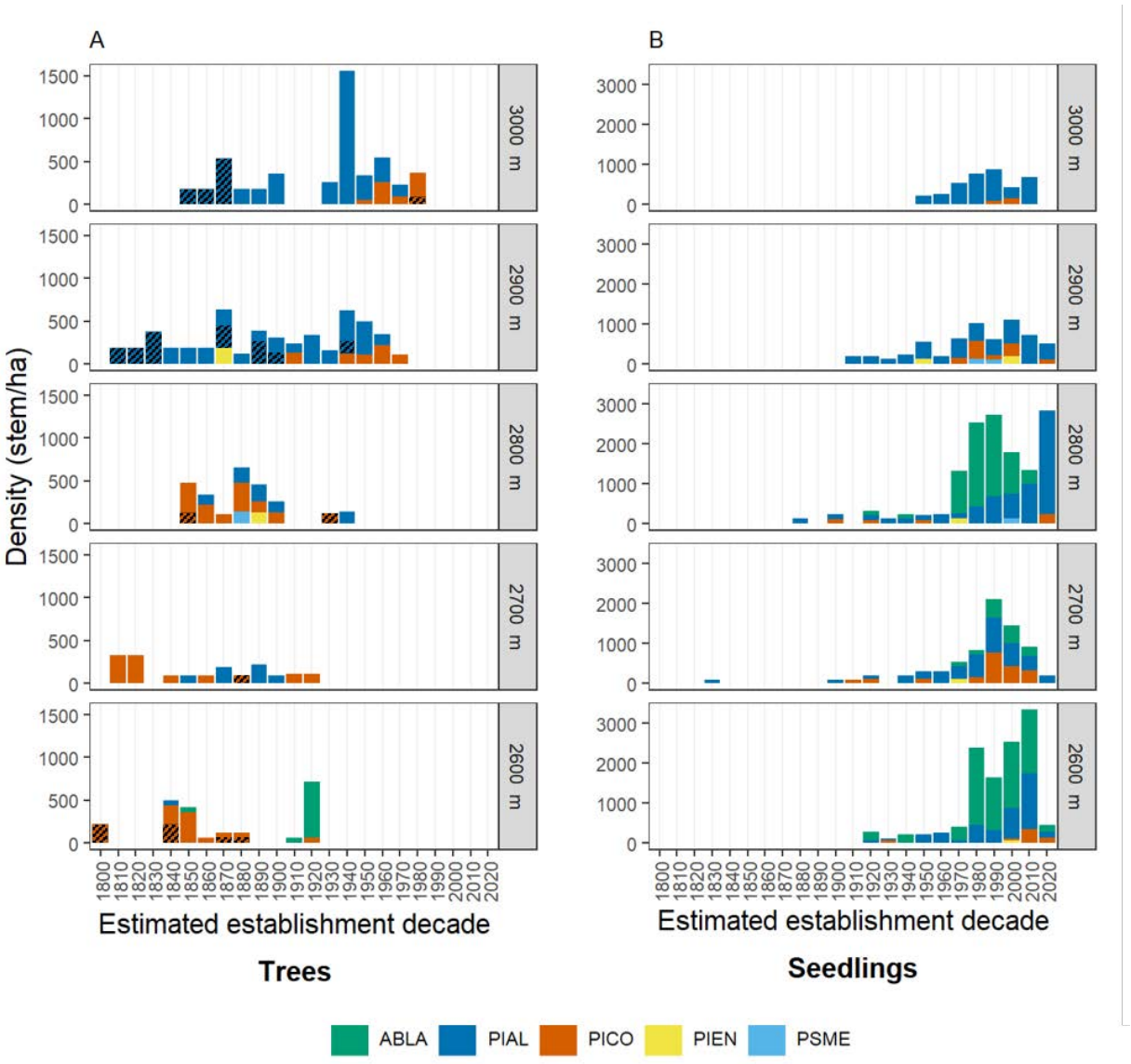

687

688 **FIGURE 2** Species-specific tree densities (stems/ha) displayed by estimated establishment year
689 decade, grouped by 100 m elevation bands for (A) live and dead (designated by black hatch
690 marks) overstory trees and (B) understory seedlings. Species codes: ABLA: *Abies lasiocarpa*;
691 PIAL: *Pinus albicaulis*; PICO: *Pinus contorta*; PIEN: *Picea engelmannii*; PSME: *Pseudotsuga*
692 *menziesii*.

693

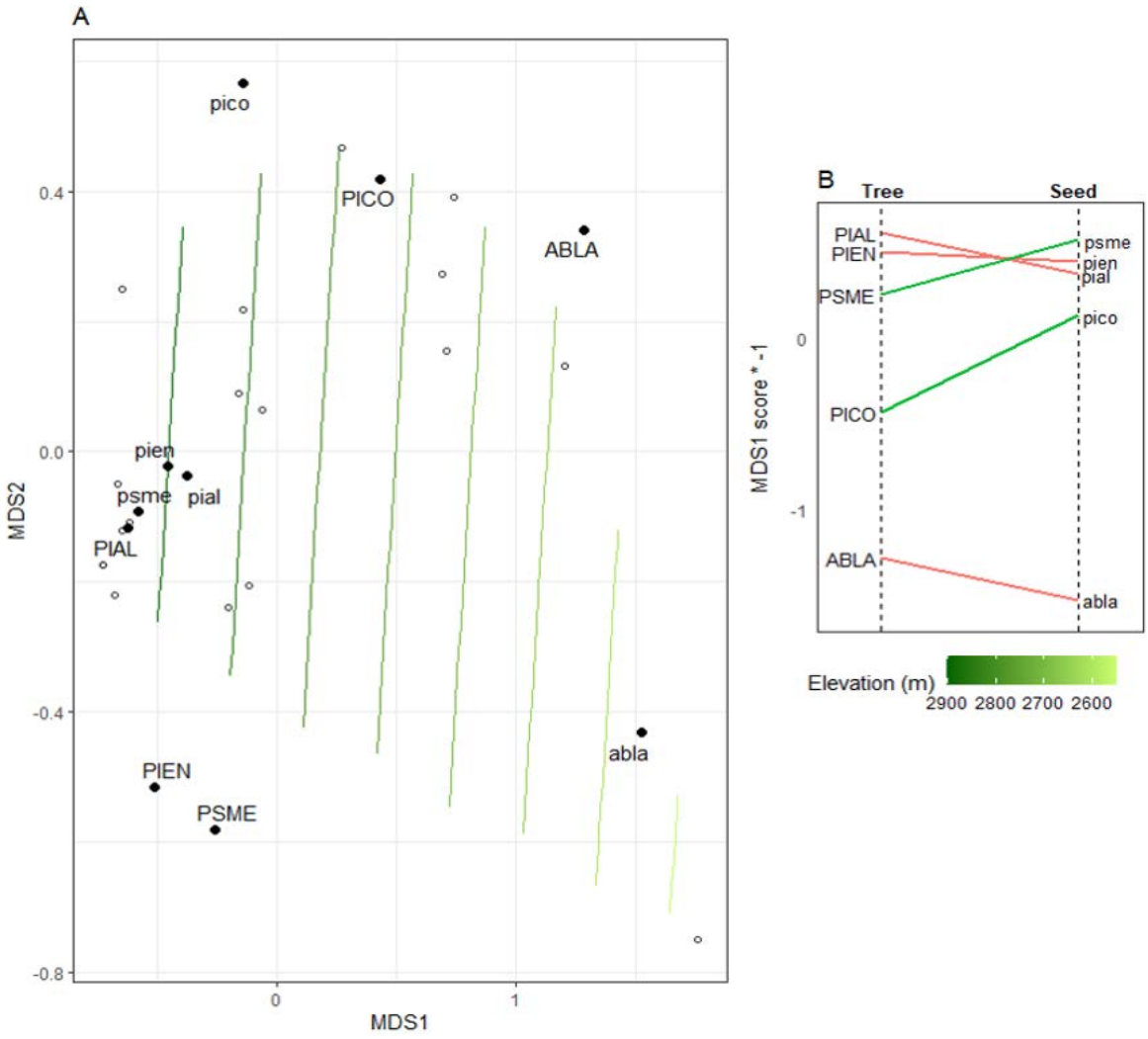

694

695 **FIGURE 3** NMDS ordination of species distributions. Overstory trees are represented by
696 capitalized species codes, while understory trees (seedlings and saplings) are represented by
697 lowercase species codes. Species codes are as follows: ABLA: *Abies lasiocarpa*; PIAL: *Pinus*
698 *albicaulis*; PICO: *Pinus contorta*; PIEN: *Picea engelmannii*; PSME: *Pseudotsuga menziesii*. (A)
699 Two-axis NMDS ordination of density (stems/ha) by species and form (overstory trees versus
700 seedlings and saplings) at each sampling plot (stress = 0.02), plotted along an elevational
701 gradient. Open circles represent plot locations, black circles represent centers of species forms
702 (trees, seedlings and saplings), and contour lines are at 50 m altitude intervals. (B) Difference

703 and magnitude in MDS scores for overstory and understory species represented by plotting
704 MDS1 scores x -1 (for ease of interpretation). For panel B, a negative slope (red) suggests the
705 center of the distribution of species seedlings is located at lower elevations than mature trees of
706 the same species, and a positive slope (green) suggests an upward shift in establishment by a
707 species.
708

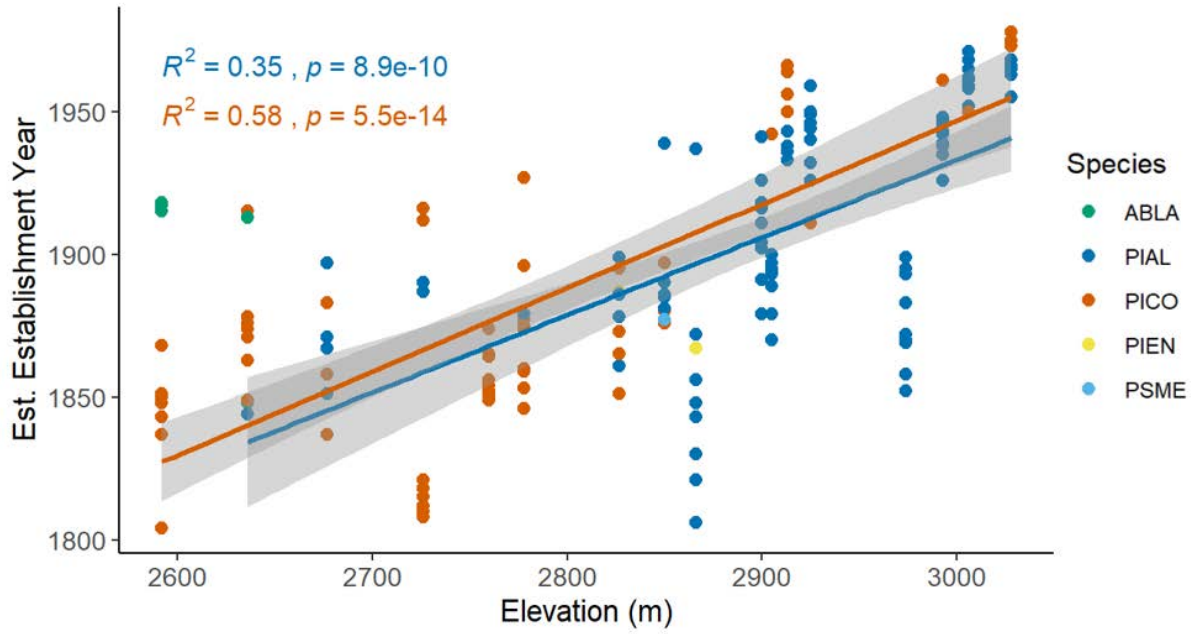

709

710 **FIGURE 4** Estimated establishment year of overstory trees by plot elevation. Regression lines

711 are shown for the two most prevalent species on the transect. Species codes: ABLA: *Abies*

712 *lasiocarpa*; PIAL: *Pinus albicaulis*; PICO: *Pinus contorta*; PIEN: *Picea engelmannii*; PSME:

713 *Pseudotsuga menziesii*.

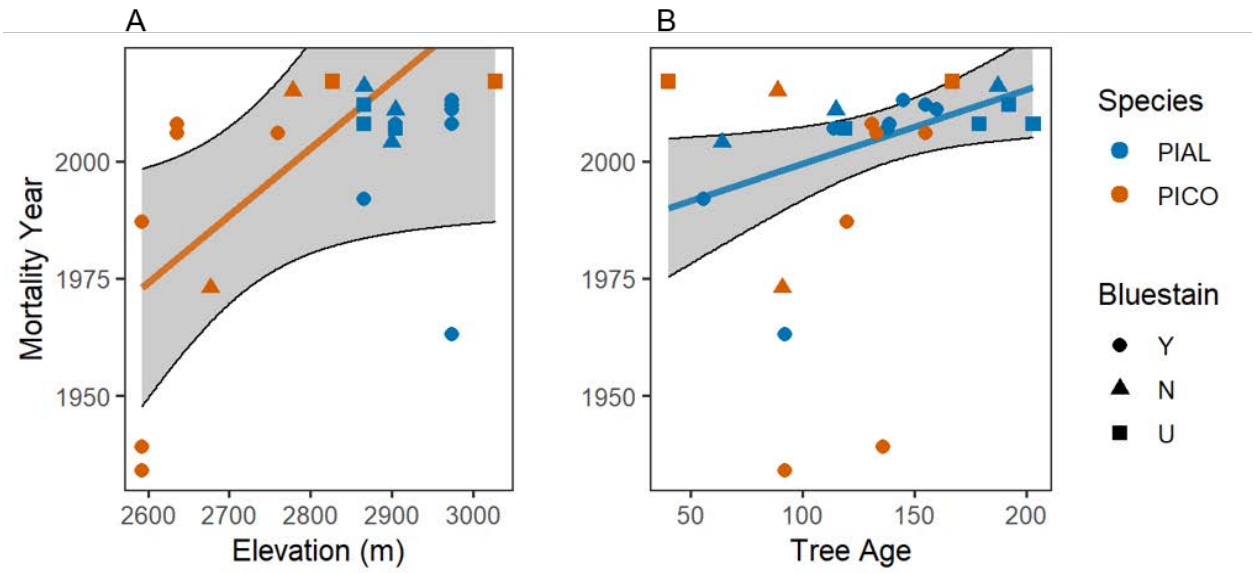

714

715 **FIGURE 5** (A) Snag mortality year (n = 26) by plot elevation. Of the five species present on the
716 transect, tree mortality was concentrated exclusively in *Pinus contorta* (PICO; n = 10) and *Pinus*
717 *albicaulis* (PIAL; n = 16). We assessed tree core samples for bluestain fungus as an indicator of
718 *Dendroctonus ponderosae* presence (Y: Yes, N: No, U: Undetermined). Mortality year had a
719 positive relationship with elevation in *P. contorta* ($p = 0.047$) and no relationship in *P. albicaulis*
720 ($p = 0.443$). (B) Snag mortality year by estimated tree age. Recent mortality events tended to
721 affect older *P. albicaulis* trees on average ($p = 0.003$).

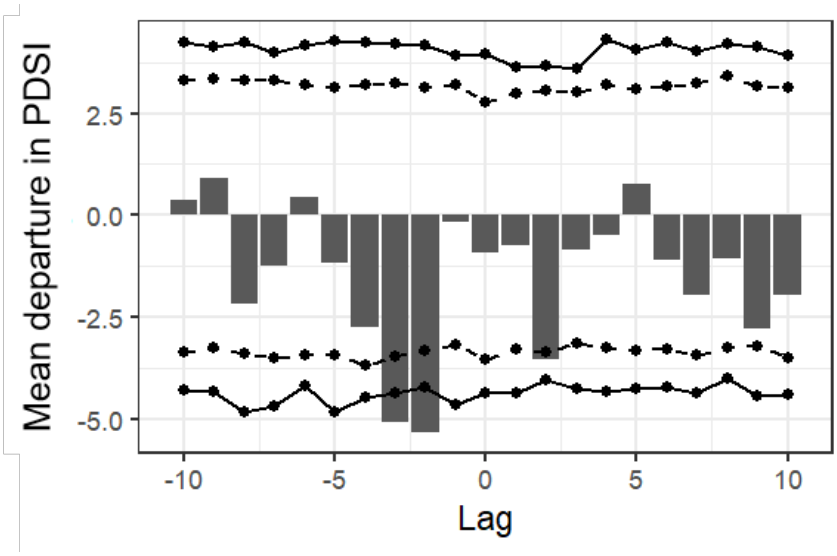

FIGURE 6 Superposed epoch analysis results of drought conditions surroundingtree mortality events (n= 26) in the study area from 1895-2019. A composite of all mortality event dates and their associated Palmer Drought Severity Index (PDSI) values (year "0") is presented with a +/- 10-year lag with 95% (dashed lines) and 99% (solid lines) bootstrapped confidence intervals. Bars represent mean departures in PDSI for the years surrounding a mortality event from mean conditions across the entire time series, with a significant departure exceeding the confidence intervals. Two to three years prior to the mortality event years, conditions were much drier than average ($p < 0.01$).

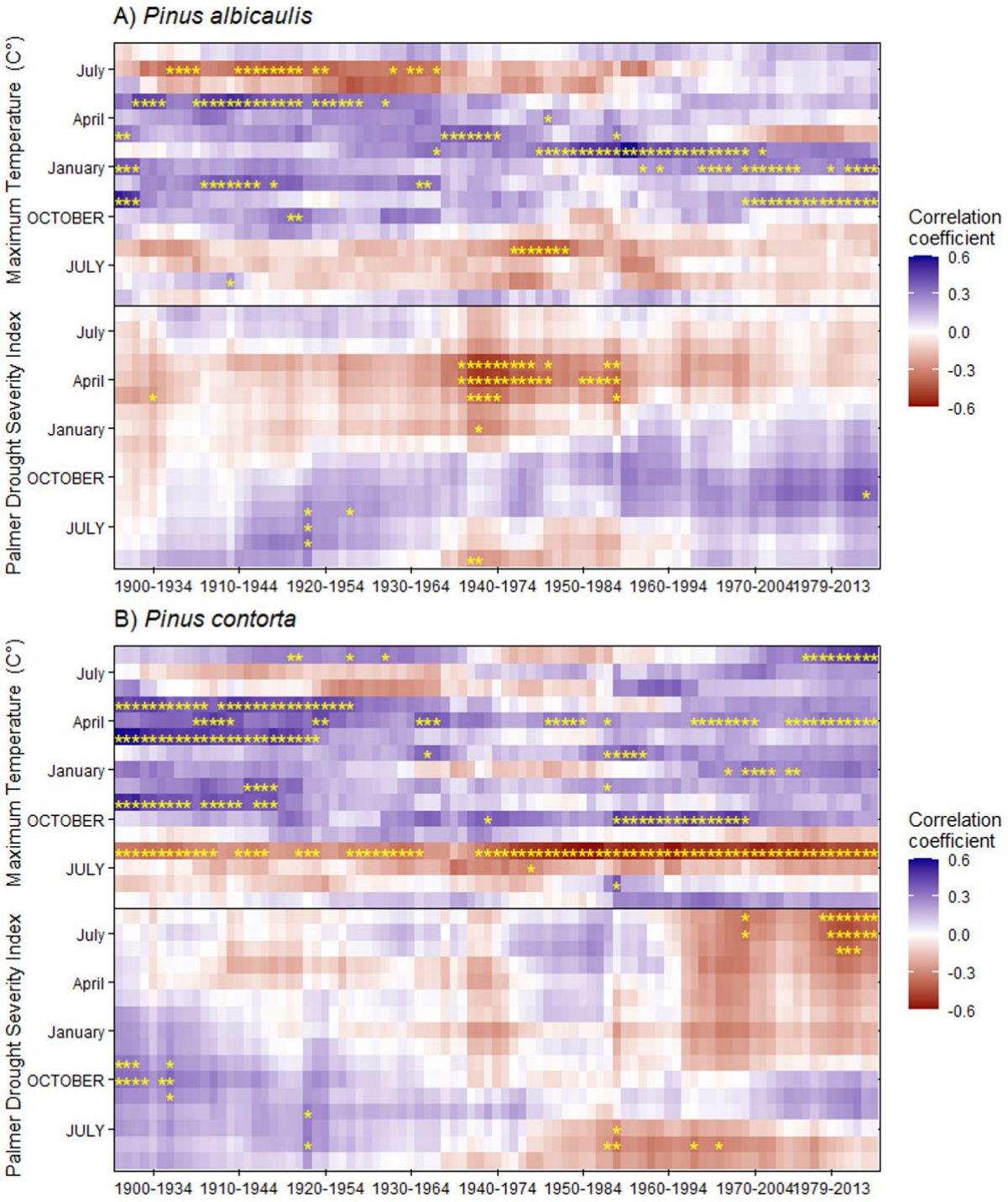

733

734 **FIGURE 7** Correlation coefficients of *Pinus albicaulis* (A) and *Pinus contorta* (B) annual ring-

735 width growth relationships to monthly maximum temperature and the Palmer Drought Severity

736 Index (PDSI), across a moving window of 35 years. Months labeled in all capital letters are from

737 the year prior to that of the ring width measurement. Asterisks indicate significance (p <0.05)

738 using the 95% percentile range method (Dixon, 2001).